ISA Transactions xxx (2018) 1–10

Contents lists available at ScienceDirect

ISA Transactions

journal homepage: www.elsevier.com/locate/isatrans

Practice article

Continuous fractional-order Zero Phase Error Tracking Control

Lu Liu [a], Siyuan Tian [b], Dingyu Xue [c], Tao Zhang [b], YangQuan Chen [d,*]

[a] School of Marine Science and Technology, Northwestern Polytechnical University, Xi'an, 710072, China
[b] Lam Research Corporation, 4650 Cushing Parkway, Fremont, CA, 94538, USA
[c] Department of Information Science and Engineering, Northeastern University, Shenyang, 110819, China
[d] Mechatronics, Embedded Systems and Automation (MESA) Lab, School of Engineering, University of California, Merced, 5200 North Lake Road, Merced, CA, 95343, USA

ARTICLE INFO

Article history:
Received 7 December 2016
Revised 4 November 2017
Accepted 15 January 2018
Available online XXX

Keywords:
Fractional calculus
Feedforward control
Tracking control
Zero-pole cancellation

ABSTRACT

A continuous time fractional-order feedforward control algorithm for tracking desired time varying input signals is proposed in this paper. The presented controller cancels the phase shift caused by the zeros and poles of controlled closed-loop fractional-order system, so it is called Fractional-Order Zero Phase Tracking Controller (FZPETC). The controlled systems are divided into two categories i.e. with and without non-cancellable (non-minimum-phase) zeros which stand in unstable region or on stability boundary. Each kinds of systems has a targeted FZPETC design control strategy. The improved tracking performance has been evaluated successfully by applying the proposed controller to three different kinds of fractional-order controlled systems. Besides, a modified quasi-perfect tracking scheme is presented for those systems which may not have available future tracking trajectory information or have problem in high frequency disturbance rejection if the perfect tracking algorithm is applied. A simulation comparison and a hardware-in-the-loop thermal peltier platform are shown to validate the practicality of the proposed quasi-perfect control algorithm.

1. Introduction

In the last few decades, the fractional calculus has attracted lots of attention in many research fields, such as physics [1], mechatronics systems [2,3], signal processing [4], biological system [5], chemistry [6], etc. Among them, fractional-order (FO) control system theory and application developed even faster. A lot of significant work aiming at FO controller design algorithm has been done in recent years [7–11]. However, most of the related studies focused on the design of FO feedback controllers. Normally, feedback controllers are aiming at regulation against disturbance input. But when perfect tracking performance is required in control loop, the FO feedforward controller will also be necessary [12].

There are mainly two kinds of trajectory tracking control: one is for tracking a given desired trajectory, and the other is for tracking an unknown trajectory [13]. In this paper, we focus on the former one with two FO controllers (i.e. a feedforward FO controller and a predesigned feedback FO controller) in the system to be controlled. The feedback FO controller is used for dynamic system performance regulation and the FO feedforward controller helps in achieving better tracking performance. The feedforward controller proposed in this paper is designed based on the system inversion theory [14]. For minimum phase systems without non-cancellable zeros and poles (zeros and poles which stand in unstable region or on stability boundary) in their closed-loop transfer functions, the inversed feedforward controller is easy to be designed. However, the design process turns to be complicated when the controlled system has non-cancellable zeros. The non-cancellable zeros will turn into unstable poles after inversion and make the whole system unstable or oscillating. This complicated inversion problem can be solved by an effective tracking control algorithm named Zero Phase Error Tracking Control (ZPETC). The ZPETC tracking algorithm which eliminated the phase error caused by non-cancellable zeros and realized a perfect tracking was put forward by Tomizuka [15]. Ever since, several effective feedforward tracking control algorithms have been proposed based on ZPETC. Torfs et al. gave more insight into ZPETC and compensated the gain error by adding additional feedforward terms [16]; Haack and Tomizuka discussed about inserting a filter before feedforward controller to improve tracking performance in Ref. [17]; a similar work which assumed there were some slowly varying parts in the closed-loop system transfer function was studied by Tsao and Tomizuka in Ref. [18]; an improved ZPETC designed without factorization of zero polynomial was proposed by Adnan et al. [19].

* Corresponding author.
E-mail addresses: liulu12201220@nwpu.edu.cn (L. Liu), siyuan.tian@lamresearch.com (S. Tian), xuedingyu@mail.neu.edu.cn (D. Xue), tao.zhang@lamresearch.com (T. Zhang), ychen53@ucmerced.edu (Y. Chen).

https://doi.org/10.1016/j.isatra.2018.01.025
0019-0578/

However, the existing ZPETC related tracking algorithms are mainly used for integer-order (IO) systems and they are unavailable to the rapid developed FO systems. In this paper, we focus on the design of continuous time Fractional-Order Zero Phase Error Tracking Controller (FZPETC) which can be applied on both IO and FO systems. Conventional ZPETC was generated in discrete-time domain, and had to be converted into continuous domain when it was applied on continuous systems. Nevertheless, thanks to the fast computational tools today, a lot of discrete time systems can be replaced by continuous time ones with high sampling frequencies [13]. Especially for FO control systems, more continuous time system transfer functions are used. This is because the conversion of FO transfer functions from continuous time domain to discrete time domain is more complicated and may not be so accurate compared with IO systems.

The FZPETC proposed in this paper is essentially a differentiator or high pass filter whose numerator order is larger than its denominator order. Therefore, future desired trajectory information is needed in the controller design process. The length of the required future desired trajectory decides by the zero locations and design specifications of the controlled system. The controlled system with the proposed feedforward FZPETC and a predesigned feedback controller is depicted in Fig. 1. The method of distinguishing cancellable zeros and non-cancellable ones and the tuning methods of FZPETC aiming at different circumstances are presented respectively. Moreover, for systems with unavailable future tracking trajectory information or having high frequency disturbance rejection problem when the perfect tracking algorithm is applied, an alternative quasi-perfect tracking control algorithm is also presented.

The following of this paper is organized as: in section 2, the stability analysis method of FO control systems is given; the detailed tuning rules of the proposed controller aiming at FO systems with cancellable zeros, with zeros on stability boundaries and with non-cancellable zeros are presented respectively in section 3; a quasi-perfect tracking algorithm is presented in section 5 for the systems which cannot satisfy the perfect tracking requirements or have problem in high frequency gain error; simulation and hardware-in-loop experiment of tracking performance of FO systems are presented in section 4 and 6 to illustrate the effectiveness of the proposed control strategy; finally, the conclusions are made in section 7.

2. Stability of fractional order system

Before discussing about the tuning rules of FZPETC, one important step is making clear of how to distinguish cancellable zeros and non-cancellable zeros in the original closed-loop system. Compared with IO control systems, the stability analysis of FO systems is quite different [20]. Several pioneer works have discussed about the stability conditions of FO control systems [20–24]. A stability analysis method of distributed parameter FO system with distributed delay has been given in Ref. [21]; stability analysis of fractional differential system using co-prime factorization algorithm was shown in Ref. [22]; in Ref. [23], the stability conditions for interval FOLTI (Fractional-Order Linear Time Invariant) system have been discussed; a numerical investigation of robust stability of FO uncertain system was discussed in Ref. [25]; the general robust stability conditions for commensurate order FO linear and nonlinear systems were proposed in Ref. [20]. Some of these stability analysis methods were put forward for specific kinds of FO systems, so an appropriate method should be chosen according to the controlled FO system. In this paper, we use the general FO linear system stability condition proposed in Ref. [20] without loss of generality.

An FO control system can be generally described by the following transfer function:

$$G(s) = \frac{b_0 s^{\beta_0} + b_1 s^{\beta_1} + \cdots + b_m s^{\beta_m}}{a_0 s^{\alpha_0} + a_1 s^{\alpha_1} + \cdots + a_n s^{\alpha_n}} = \frac{N(s)}{D(s)}, \tag{1}$$

where, $a_0, a_1, \ldots, a_n$ and $b_0, b_1, \ldots b_m$ are constants which represent the coefficients of denominator and numerator; $\alpha_0, \alpha_1, \ldots, \alpha_n$ ($\alpha_0 < \alpha_1 < \cdots < \alpha_n$) and $\beta_0, \beta_1, \ldots, \beta_m$ ($\beta_0 < \beta_1 < \cdots < \beta_m$) are arbitrary real number orders of denominator and numerator respectively.

The incommensurate order system in Equation (1) can be transformed into a commensurate one as [26]:

$$G'(s) = \frac{b_0 + b_1 s^{1/\mu} + \cdots + b_m s^{m/\mu}}{a_0 + a_1 s^{1/\mu} + \cdots + a_n s^{n/\mu}}, \quad (\mu > 1). \tag{2}$$

It should be remarked here that most FO systems can be expressed as Equation (2) [20]. The definition of $G'(s)$ has one Riemann surface with μ Riemann sheets [27].

Generally, set $\omega = s^{1/\mu}$, then the transfer function with operator s in s-domain can be transformed into a complex ω-domain with μ sheets in Riemann surface [20]. The original principal sheet of Riemann surface is defined as $-\pi < \arg(s) < \pi$. However, after the mapping of $\omega = s^{1/\mu}$, the corresponding principal sheet transforms into $-\pi/\mu < \arg(\omega) < \pi/\mu$. Namely, the right half unstable boundary in s-domain becomes $-\pi/2\mu < \arg(\omega) < \pi/2\mu$ in ω-domain. That is to say, in s-domain, a stable system will not have right half poles. But in ω-domain, right half poles may exist in stable system as shown in Fig. 2.

Consider an FO pseudo-polynomial as:

$$\begin{aligned} D(s) &= c_1 s^{q_1} + c_2 s^{q_2} + \cdots + c_k s^{q_k} \\ &= c_1 s^{u_1/\mu} + c_2 s^{u_2/\mu} + \cdots + c_k s^{u_k/\mu} \\ &= c_1 (s^{1/\mu})^{u_1} + c_2 (s^{1/\mu})^{u_2} + \cdots + c_k (s^{1/\mu})^{u_k} \end{aligned}, \tag{3}$$

where, q_i ($i = 1, 2, \ldots, k$) $= \mu_i/\mu$ ($i = 1, 2, \ldots, k$) and $1/\mu$ is the greatest common divisor of q_i [28]. Hence, the fractional degree (FDEG) of polynomial $D(s)$ is got as [28]:

$$\mathrm{FDEG}\{D(s)\} = \max\{\mu_1, \mu_2, \ldots, \mu_k\}.$$

Then, the number of roots of $D(s)$ in Equation (3) can be got from the following proposition:

Proposition 1. [29]: Let $D(s)$ be an FO polynomial with $\mathrm{FDEG}\{D(s)\} = n$, then the equation $D(s) = 0$ has exactly n roots on the Riemann surface.

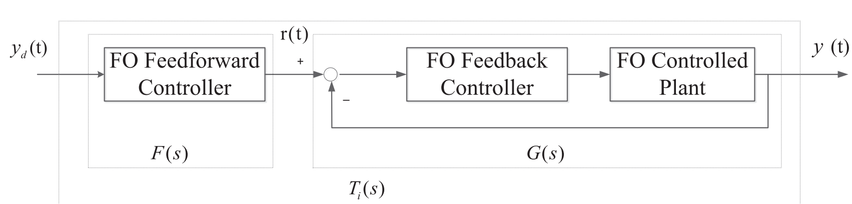

Fig. 1. Fractional order control system with feedforward and feedback controllers.

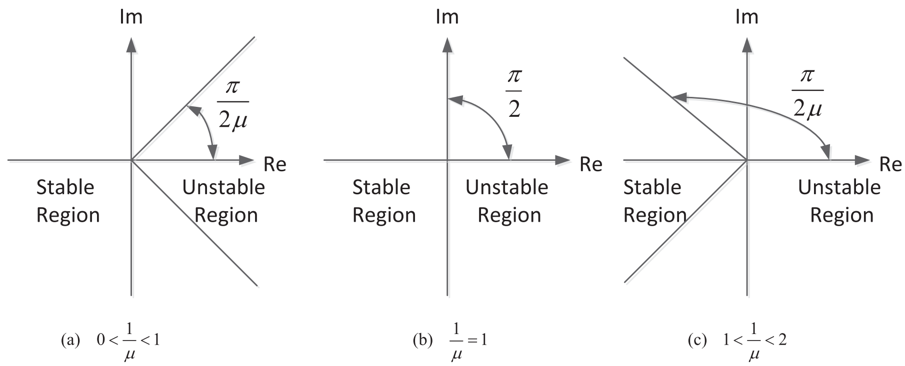

Fig. 2. Stability regions of FO system.

For FOLTI commensurate order system whose poles are in general complex conjugate, the stability condition can be stated as:

Theorem 1. [20]: A commensurate order system described by a rational transfer function:

$$G(\omega) = \frac{N(\omega)}{D(\omega)},$$

where, $\omega = s^{1/\mu}$, $\mu \in R^{+}$, $(0 < 1/\mu < 2)$, is stable if only if

$$|\arg(\omega_i)| > \frac{\pi}{2\mu},$$

with $\forall \omega_i \in C$ $(i \le n, n = \mathrm{FDEG}\{D(s)\})$ the i-th root of $D(\omega) = 0$.

3. Continuous fractional order Zero Phase Error Tracking Controller

For system with a zero/pole cancellation feedforward controller, the zeros of the controlled system will become the poles of the designed controller. In this paper, zeros of the closed-loop system which exist out of the stable area or stand on the stability boundary in theorem 1 are called non-cancellable zeros, and the others are called cancellable zeros correspondingly. Since these non-cancellable zeros will bring unstable or oscillating performance into the system and they cannot be cancelled by feedforward controller directly, the controller design methods of the systems with and without non-cancellable zeros are different.

3.1. FZPETC for FO system without non-cancellable closed-loop zeros

Consider an FO system whose closed-loop transfer function is expressed as Equation (1). It should be noted that the transfer function already includes the controlled plant and feedback controller. The relationship between the reference input signal $R(s)$ and actual output signal $Y(s)$ can be yielded as:

$$Y(s) = G(s)R(s). \quad (4)$$

Suppose there is a feedforward tracking controller with the following form:

$$R(s) = F(s)Y_d(s) = \frac{D(s)}{N(s)}Y_d(s), \quad (5)$$

where, $Y_d(s)$ is the desired output. Thus, when the initial conditions are zero, the overall transfer functional of the system is $Y(s) = Y_d(s)$. This means the controlled system can provide perfect tracking performance without any error. So Equation (5) gives the formulation of FZPETC for system without non-cancellable zeros. Note that if there is a delay term in $G(s)$, $Y_d(s)$ should have the same length ahead signal in order to compensate the delay. However, it has already been pointed out in Ref. [15] that if there is any non-cancellable zero in $G(s)$, the output of the system with the reference signal in Equation (5) will explode or oscillate. Even if all the zeros are in the stable area, the zeros located on the stability boundary may make the output highly oscillate.

3.2. FZPETC for FO system with non-cancellable closed-loop zeros

The non-cancellable closed-loop zeros cannot be inversed directly in neither continuous time domain nor discrete time domain. Therefore, the remained non-cancellable zeros will bring undesirable tracking error including phase error and gain error into the system. The feedforward controller tuning method for this kind of system will be more complex than that of system without non-cancellable zeros.

Also consider the closed-loop system in Equation (1), and here we factorize the numerator $N(s)$ into two parts as below:

$$N(s) = N^a(s)N^u(s), \quad (6)$$

where,

$$N^a(s) = b_0^a s^{\beta_0^a} + b_1^a s^{\beta_1^a} + \cdots + b_{m-k}^a s^{\beta_{m-k}^a} \quad (\textit{cancellable zeros}),$$

$$N^u(s) = b_0^u s^{\beta_0^u} + b_1^u s^{\beta_1^u} + \cdots + b_k^u s^{\beta_k^u} \quad (\textit{non}-\textit{cancellable zeros}),$$

k, $m \in R^{+}$, $k \le m$. Therefore, all the cancellable closed-loop zeros which will become the poles of the feedforward controller are included in $N^a(s)$, and $N^u(s)$ contains the other non-cancellable ones.

Thus, the tracking controller which can cancel all the cancellable zeros can be achieved as:

$$R(s) = F(s)Y_d(s) = \frac{D(s)}{N^a(s)N^u(1)}Y_d(s), \quad (7)$$

where, $N^u(1)$ is a scaler which is equal to the steady state gain of the closed-loop system. So that the gain error will be eliminated. Then, for zero initial state, substitute Equation (7) into Equation (4), and the overall system transfer function is obtained as:

$$Y(s) = \frac{N^u(s)}{N^u(1)}Y_d(s). \quad (8)$$

If Equation (7) is used as the feedforward controller, phase error will still exist in Equation (8). The tracking performance is not perfect. So a controller which can eliminate phase error in Equation (8) will be needed. When talking about phase error problem, the system should be transferred into frequency domain first. Transfer Equation (8) into frequency domain by substituting $j\omega$ for s as:

$$Y(j\omega) = \frac{N^u(j\omega)}{N^u(1)}Y_d(j\omega). \quad (9)$$

Please cite this article in press as: Liu L, et al. Continuous fractional-order Zero Phase Error Tracking Control, ISA Transactions (2018), https://doi.org/10.1016/j.isatra.2018.01.025

ARTICLE IN PRESS

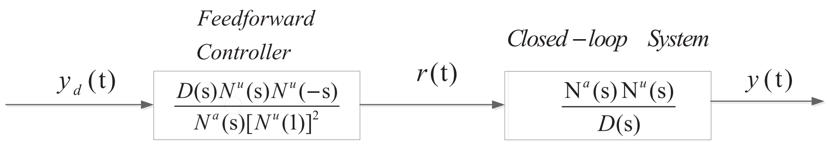

Fig. 3. FZPETC algorithm for FO system with non-cancellable zeros.

From Equation (9), it is clear that the phase error is generated by $H(j\omega) = N^u(j\omega)/N^u(1)$.

Then $H(j\omega)$ can be written as:

$$H(j\omega) = \text{Re}[H(j\omega)] + j\text{Im}[H(j\omega)], \tag{10}$$

where, $\text{Re}[H(j\omega)]$ and $\text{Im}[H(j\omega)]$ are the real and imaginary parts of $H(j\omega)$ respectively. Then, by using Euler's function, it has:

$$\begin{aligned}(j\omega)^\alpha &= \left[\omega\left(\cos\frac{\pi}{2} + j\sin\frac{\pi}{2}\right)\right]^\alpha = \left(\omega e^{\frac{\pi}{2}j}\right)^\alpha \\ &= \omega^\alpha e^{\frac{\alpha\pi}{2}j} = \omega^\alpha\left(\cos\frac{\alpha\pi}{2} + j\sin\frac{\alpha\pi}{2}\right), \\ (-j\omega)^\alpha &= \left[\omega\left(\cos\left(-\frac{\pi}{2}\right) + j\sin\left(-\frac{\pi}{2}\right)\right)\right]^\alpha = \left(\omega e^{-\frac{\pi}{2}j}\right)^\alpha \\ &= \omega^\alpha e^{-\frac{\alpha\pi}{2}j} = \omega^\alpha\left(\cos(-\frac{\alpha\pi}{2}) + j\sin\left(-\frac{\alpha\pi}{2}\right)\right) \\ &= \omega^\alpha\left(\cos\frac{\alpha\pi}{2} - j\sin\frac{\alpha\pi}{2}\right),\end{aligned}$$

where, $\text{Re}[H(j\omega)]$ and $\text{Im}[H(j\omega)]$ can be obtained as:

$$\begin{aligned}\text{Re}[H(j\omega)] &= \frac{(b_0^u\omega^{\beta_0^u}\cos\frac{\beta_0^u\pi}{2} + b_1^u\omega^{\beta_1^u}\cos\frac{\beta_1^u\pi}{2} + \cdots + b_k^u\omega^{\beta_k^u}\cos\frac{\beta_k^u\pi}{2})}{(b_0^u + b_1^u + \cdots + b_k^u)}, \\ \text{Im}[H(j\omega)] &= \frac{(b_0^u\omega^{\beta_0^u}\sin\frac{\beta_0^u\pi}{2} + b_1^u\omega^{\beta_1^u}\sin\frac{\beta_1^u\pi}{2} + \cdots + b_k^u\omega^{\beta_k^u}\sin\frac{\beta_k^u\pi}{2})}{(b_0^u + b_1^u + \cdots + b_k^u)}.\end{aligned} \tag{11}$$

Then, we get $H(-j\omega) = \text{Re}[H(j\omega)] - j\text{Im}[H(j\omega)]$, where $\text{Re}[H(j\omega)]$, $\text{Im}[H(j\omega)]$ are also given by Equation (11). Therefore,

$$H(j\omega)H(-j\omega) = Re[H(j\omega)]^2 + \text{Im}[H(j\omega)]^2. \tag{12}$$

Notice that Equation (12) does not have an imaginary part. It means that there is no phase shift introduced by Equation (12). So if Equation (12) is the overall transfer function from $Y_d(s)$ to $Y(s)$, the phase error will be zero. On the whole, the FZPETC feedforward controller can be expressed as depicted in Fig. 3 as:

$$R(s) = F(s)Y_d(s) = \frac{D(s)N^u(s)N^u(-s)}{N^a(s)[N^u(1)]^2}Y_d(s). \tag{13}$$

Three remarks should be put here in respect of the FZPETC proposed in Equation (5) and Equation (13):

1. If there is a delay term in $G(s)$, $Y_d(s)$ should have the same length ahead signal to compensate the delay.
2. The order of the numerator of FZPETC may be greater than that of the denominator. This implies that FZPETC may act as a kind of differentiator and may utilize the further desired trajectory information. Thus the desired tracking signal should be known. Moreover, as the same to other differentiators, system controlled by FZPETC may be sensitive to noise [13]. However, it will not be a problem if the reference signal is known as a smooth function. We will also propose a quasi-perfect tracking scheme in the later section to help solve the high frequency disturbance rejection problem.
3. It has already been discussed in Ref. [15] that if the desired tracking input is a sinusoidal signal with high frequency, the gain error may also be taken into consideration. It may be eliminated by a scaler $1/[Re[H(j\omega)]^2 + \text{Im}[H(j\omega)]^2]$ with $\text{Re}[H(j\omega)]$, $\text{Im}[H(j\omega)]$ given in Equation (11). Furthermore, it was pointed out in Ref. [13] that the gain error would become larger in high frequency if the input signal includes different frequency components. This may cause velocity error in point-to-point motion control process when fast tracking applies. The authors of Ref. [13] have put forward a compensated way aiming at this problem, and it may be a further research orientation of FZPETC.

4. Simulation

In this section, three different kinds of FO closed-loop systems (i.e. FO system with cancellable zeros, FO system with zeros on stability boundary, FO system with non-cancellable zeros) are used to verify the effectiveness of the proposed FZPETC algorithm. The simulation can be accomplished with the help of the tools introduced in Ref. [30].

4.1. FO system with cancellable zeros

Consider an FO system with closed-loop transfer function as:

$$G_1(s) = \frac{s^{2.4} + 1.8s^{1.6} + 1.2006s^{0.8} + 0.57675}{s^{3.2} + 1.2s^{2.4} + 3.02s^{1.6} + 4.396s^{0.8} + 2.1389}, \tag{14}$$

where, $D(s) = s^{3.2} + 1.2s^{2.4} + 3.02s^{1.6} + 4.396s^{0.8} + 2.1389$. Since the denominator does not need to be factorized in the presented control scheme, all the denominators of the closed-loop systems discussed in this section will be the same. This will make readers understand the proposed control algorithm for different types of systems easily.

According to section 2, the incommensurate order system in Equation (14) can be transformed into a commensurate one as:

$$G_1(s) = \frac{(s^{0.8})^3 + 1.8(s^{0.8})^2 + 1.2006s^{0.8} + 0.57675}{(s^{0.8})^4 + 1.2(s^{0.8})^3 + 3.02(s^{0.8})^2 + 4.396s^{0.8} + 2.1389}, \tag{15}$$

so that we can set $\omega = s^{0.8}$ with $\mu = 1.25$ to transform the transfer function from s-domain into ω-domain:

$$G_1(\omega) = \frac{\omega^3 + 1.8\omega^2 + 1.2006\omega + 0.57675}{\omega^4 + 1.2\omega^3 + 3.02\omega^2 + 4.396\omega + 2.1389}. \tag{16}$$

According to Proposition 1 and Theorem 1, the system has four poles i.e. $P_{1,2} = 0.2 \pm 1.7j$, $P_{3,4} = -0.8 \pm 0.3j$ and three zeros i.e. $Z_1 = -1.2$, $Z_2 = -0.3 \pm 1.7j$, and the stability boundary is $|\arg\omega_i| > \frac{\pi}{2\times1.25} = \frac{2}{5}\pi$. The stability boundary and poles, zeros positions are shown in Fig. 4. Clearly from Fig. 4, the system does not have any non-cancellable pole or zero.

After making clear of the controlled closed-loop system type, we can design the FZPETC referring to Equation (5) in section 3-A as:

$$R(s) = \frac{s^{3.2} + 1.2s^{2.4} + 3.02s^{1.6} + 4.396s^{0.8} + 2.1389}{s^{2.4} + 1.8s^{1.6} + 1.2006s^{0.8} + 0.57675}Y_d(s), \tag{17}$$

where, $Y_d(s)$ is the Laplace transform of the desired tracking signal $y_d(t) = 1.3\ \sin(t + \frac{\pi}{6})$.

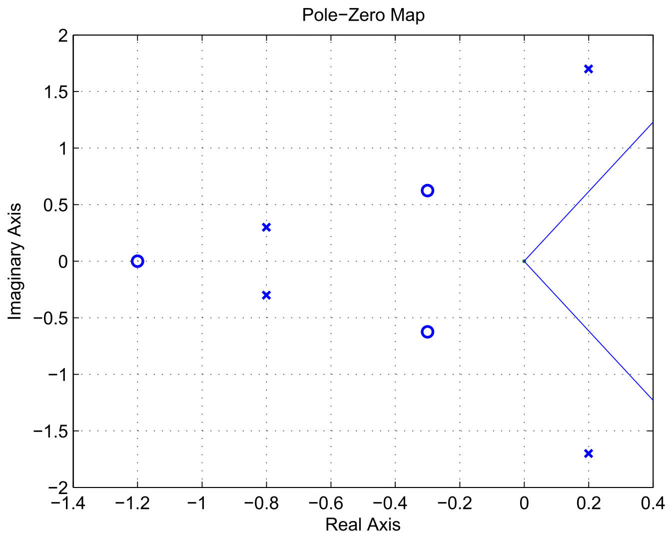

Fig. 4. Pole-zero locations of $G_1(\omega)$ ('×' stands for pole and '∘' stands for zero).

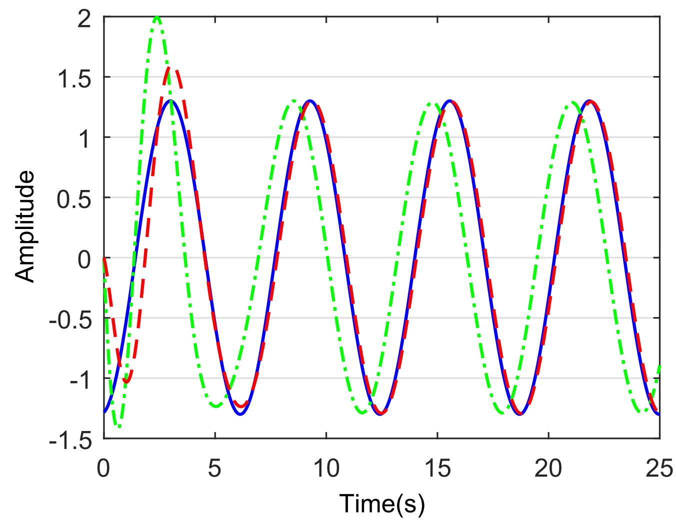

Fig. 6. Tracking performance comparison of $G_1(s)$ (solid line stands for reference, green dash line stands for $G_1(s)$, and red dash line stands for $G_1(s)$ + FZPETC).

The phase and tracking performance comparisons of $G_1(s)$ with and without the proposed FZPETC are depicted in Fig. 5 and Fig. 6 respectively. Similar to Fig. 4 in Ref. [15], the phase shift turns into zero for all frequencies. It also means that there will not have any phase error between the desired tracking signal and actual output signal. From Fig. 6, it is shown that the tracking performance of the controlled system with FZPETC has almost no error in both phase and amplitude. However, the tracking performance of the original closed-loop system seems a little off in both aspects.

4.2. FO system with zeros on stability boundary

The closed-loop system to be controlled in this subsection is:

$$G_2(s) = \frac{s^{2.4} + 0.4s^{1.6} + 0.71536s^{0.8} + 2.0104}{D(s)}. \tag{18}$$

Obviously, the poles of $G_2(s)$ in Equation (18) are the same with that of $G_1(s)$ in Equation (14) as well as the commensurate transform operator $\omega = s^{0.8}$ with $\mu = 1.25$. So $G_2(s)$ can be transformed into ω-domain as:

$$G_2(\omega) = \frac{\omega^3 + 0.4\omega^2 + 0.71536\omega + 2.0104}{\omega^4 + 1.2\omega^3 + 3.02\omega^2 + 4.396\omega + 2.1389}. \tag{19}$$

Moreover, because of the same transform operator, the stability boundary of $G_2(s)$ will also be the same with $G_1(s)$. From Equation (19), the zeros of $G_2(s)$ can be got as $Z_1 = -1.2, Z_{2,3} = -0.4 \pm 1.231j$, and the pole-zero map plot is given in Fig. 7. Unfortunately, different from $G_1(s)$, $G_2(s)$ has two zeros i.e. $Z_{2,3} = -0.4 \pm 1.231j$ standing on the stability boundary. It means the system cannot be inverted directly. Therefore, we first change Equation (18) into zero-pole form as:

$$G_2(s) = \frac{(s^{0.8} + 1.2)(s^{0.8} - 0.4 + 1.231j)(s^{0.8} - 0.4 - 1.231j)}{D(s)}, \tag{20}$$

then, the feedforward controller proposed in this paper can be achieved based on Equation (13) as:

$$R(s) = \frac{D(s)(s^{0.8} - 0.5)(-s^{0.8} - 0.5)\ldots}{(s^{0.8} + 0.4 + 0.7j)(s^{0.8} + 0.4 - 0.7j)\ldots} \cdot \frac{(-s^{0.8} - 0.4 + 1.231j)(-s^{0.8} - 0.4 - 1.231j)}{[(1^{0.8} - 0.4 + 1.231j)(1^{0.8} - 0.4 - 1.231j)]^2} Y_d(s), \tag{21}$$

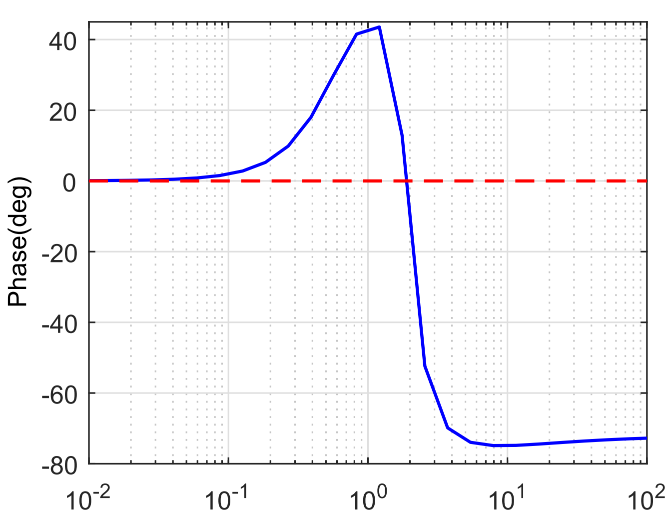

Fig. 5. Phase comparison of $G_1(s)$ (solid line stands for original $G_1(s)$, and dash line stands for $G_1(s)$ + FZEPTC).

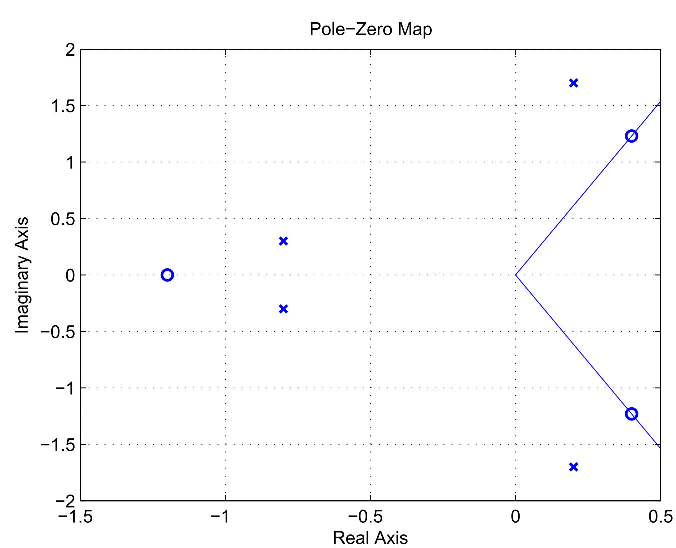

Fig. 7. Pole-zero locations of $G_2(\omega)$ ('×' stands for pole and '∘' stands for zero).

Please cite this article in press as: Liu L, et al. Continuous fractional-order Zero Phase Error Tracking Control, ISA Transactions (2018), https://doi.org/10.1016/j.isatra.2018.01.025

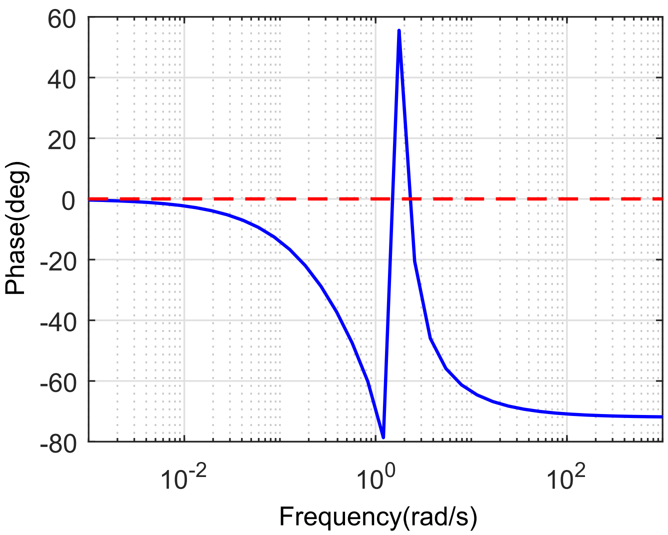

Fig. 8. Phase comparison of $G_2(s)$ (solid line stands for original $G_2(s)$, and dash line stands for $G_2(s)$ + FZEPTC).

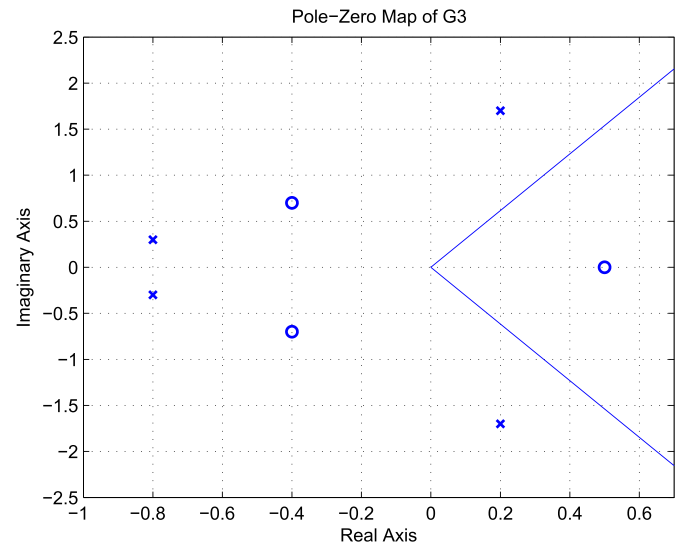

Fig. 10. Pole-zero locations of $G_3(\omega)$ ('×' stands for pole and '∘' stands for zero).

where, $Y_d(s)$ is the same with that of Equation (17).

Fig. 8 and Fig. 9 show the comparisons of phase and tracking performance with and without FZPETC of $G_2(s)$. The closed-loop system with the proposed FZPETC still gives almost perfect tracking performance in Fig. 9. The amplitude of the system without FZPETC is right, but the phase error is relatively large. Moreover, the beginning of the tracking trajectory of the system without FZPETC oscillates severely.

4.3. FO system with non-cancellable zeros

The closed-loop system discussed in this subsection also has the same denominator in its transfer function as the systems considered above:

$$G_3(s) = \frac{s^{2.4} + 0.3s^{1.6} + 0.25s^{0.8} - 0.325}{D(s)}. \quad (22)$$

Therefore, it also has the same poles, transform operator and stability boundary as $G_1(s)$ and $G_2(s)$, and the ω-domain $G_3(\omega)$ can be obtained as:

$$G_3(\omega) = \frac{\omega^3 + 0.3\omega^2 + 0.25\omega - 0.325}{\omega^4 + 1.2\omega^3 + 3.02\omega^2 + 4.396\omega + 2.1389}. \quad (23)$$

Fig. 10 illustrates the zero-pole locations of $G_3(s)$ and shows that there is one non-cancellable zero in the three zeros of the system i.e $Z_1 = -0.5$, $Z_2 = -0.4 \pm 0.7j$. Obviously, the former one is a non-cancellable zero. Then, factorize the numerator of $G_3(s)$ as:

$$G_3(s) = \frac{(s^{0.8} - 0.5)(s^{0.8} + 0.4 + 0.7j)(s^{0.8} + 0.4 - 0.7j)}{D(s)}. \quad (24)$$

Therefore, the proposed FZPETC can be achieved as:

$$R(s) = \frac{D(s)(s^{0.8} - 0.5)(-s^{0.8} - 0.5)}{(s^{0.8} + 0.4 + 0.7j)(s^{0.8} + 0.4 - 0.7j)(1^{0.8} - 0.5)^2} Y_d(s), \quad (25)$$

where, the expression of $Y_d(s)$ is the same to that in Equations (17) and (21).

The phase comparison of $G_3(s)$ in Fig. 11 shows zero shift of system with FZPETC as expected. The sinusoidal tracking performance with FZPETC in Fig. 12 also performs much better compared with

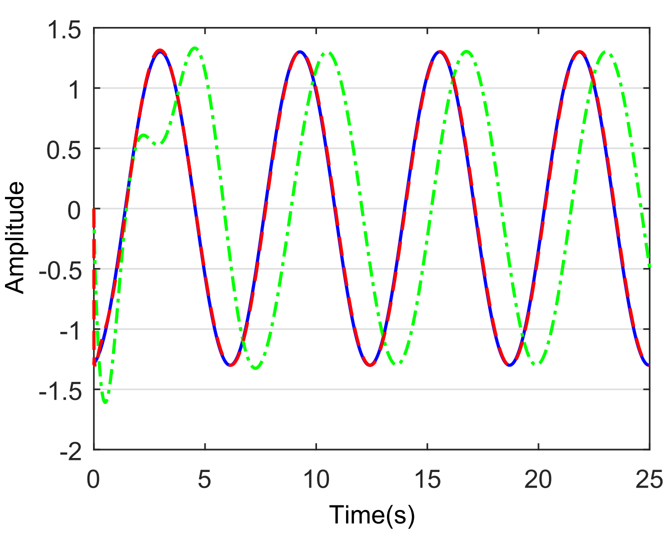

Fig. 9. Tracking performance comparison of $G_2(s)$ (solid line stands for reference, green dash line stands for $G_2(s)$, and red dash line stands for $G_2(s)$ + FZPETC).

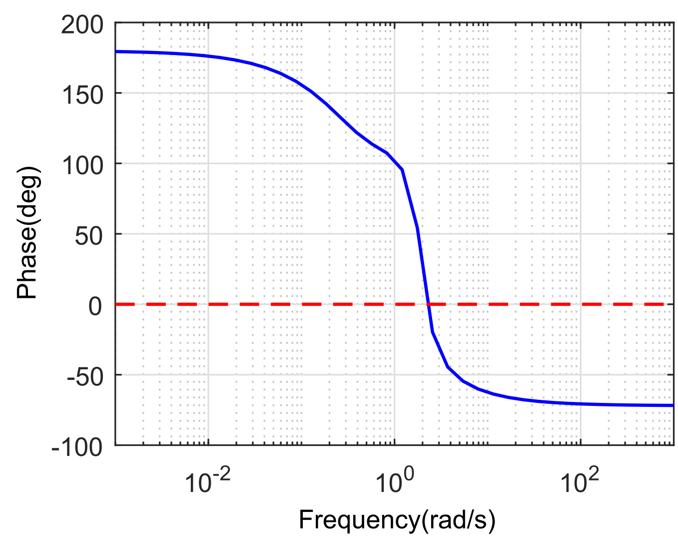

Fig. 11. Phase comparison of $G_3(s)$ (solid line stands for original $G_3(s)$, and dash line stands for $G_3(s)$ + FZEPTC).

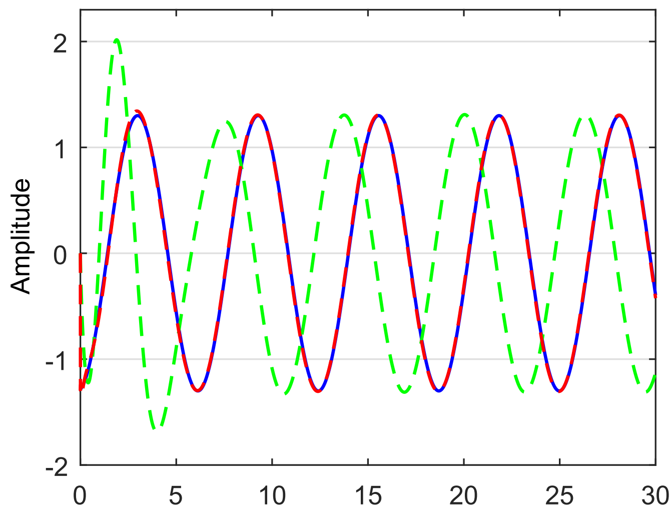

Fig. 12. Tracking performance comparison of $G_3(s)$ (solid line stands for reference, green dash line stands for $G_3(s)$, and red dash line stands for $G_3(s)$ + FZPETC).

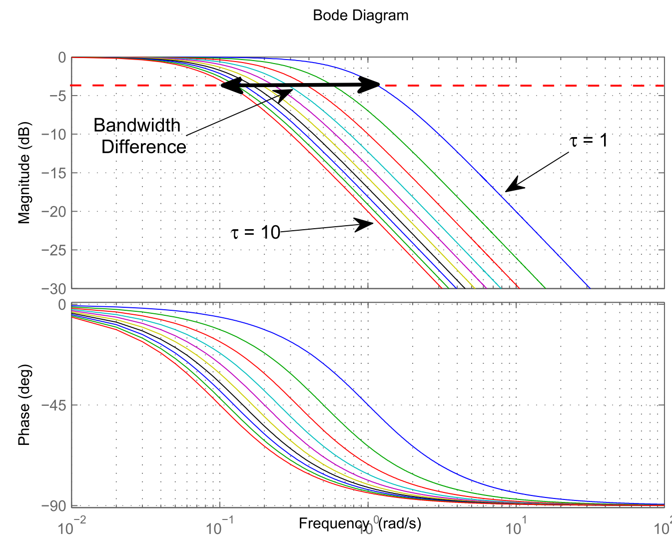

Fig. 13. Different closed-loop bandwidths with different τ.

that without FZEPTC. A problem which occurs in last subsection also appears here that the beginning part of the system without FZPETC oscillates a lot. But this does not happen in that of the system with FZPETC. On a whole, it is verified from the simulation results that the proposed FZPETC can help systems with and without non-cancellable zeros achieve satisfactory tracking performances.

5. Quasi-perfect tracking

The perfect tracking algorithm for FO system has been discussed in the above sections. However, perfect tracking is an ideal performance which may be quite hard to be achieved in practice. This is because the improper expressions in Equation (5) and Equation (13) are hard to obtain in some practical situations. Moreover, the perfect tracking controller may bring some aggressive behaviours to the system. The controlled system may also be quite sensitive to high frequency disturbance. In this section, a quasi-perfect tracking algorithm which gives an alternative option in achieving better tracking performance in high frequency is proposed. This algorithm is also effective in dealing with the improper problem.

In section 3, the overall transfer function $T_i(s)$ in Fig. 1 was made equal to 1, so that the output signal would track the reference signal perfectly. But this may need an improper feedforward controller and may bring in some problems to the system in high frequency as mentioned above. Here, we make a trade off between the perfect tracking performance and the problems by setting $T_i(s)$ as:

$$T_i(s) = F(s)G(s) = \left(\frac{1}{\tau s + 1}\right)^{\alpha}, \tag{26}$$

where α can be an arbitrary order, τ is defined by users, and $F(s)$ is achieved according to Equation (5) or Equation (13). In this way, the improper problem is solved and the a quasi-perfect tracking can be achieved by tuning α and τ in Equation (26). We suggest to set the order α between 0.8 and 1.5, so that a better performance with lower overshoot and smaller rise time can be achieved. Taking $\alpha = 1$ in Equation (26) for example, Fig. 13 shows the closed-loop bandwidth difference between systems with $\tau = 1$ to $\tau = 10$. It is illustrated that the bandwidth of the overall system can be adjusted by τ, which also means the rise time and tracking performance can be improved by changing the values of α and τ. Moreover, in normal condition, the amplitude of the system at high frequency will drop rapidly to avoid high frequency disturbance. But if the overall transfer function in Fig. 1 is set to 1, the amplitude of the system in high frequency may increase rapidly. This will bring troubles into the system. However, this problem can be solved by setting α in Equation (26) into different values, so that the slope of the amplitude curve of the system in frequency domain can be set into -20α dB to avoid high frequency disturbance.

In order to verify the effectiveness of the quasi-perfect FZPETC tracking algorithm proposed in this section, a simulation comparison is accomplished. The controlled system is a tractor with the transfer function $P(s)$ shown in Ref. [31].

$$P(s) = \frac{4.9}{s^2(s^2 + 3.57s + 11.36)}. \tag{27}$$

The unit step input tracking performance comparison of the system shown in Equation (27) controlled by three different controllers, namely the PD controller (P = 0.01, D = 3), PD$^{\mu}$ controller (P = 0.011, D = 3.3, μ = 1.0865) designed in Ref. [31] and the quasi-perfect FZPETC proposed in this section, is shown in Fig. 14. The parameters of $T_i(s)$ in Equation (26) are chosen as $\tau = 0.1$ and $\alpha = 3$. Fig. 15 gives the corresponding closed-loop bandwidth comparison. From Fig. 14, it can be seen that the control performance of the system controlled by FZPETC outperforms the other two in terms of smaller rise time and overshoot. The wider closed-loop bandwidth in Fig. 15 also val-

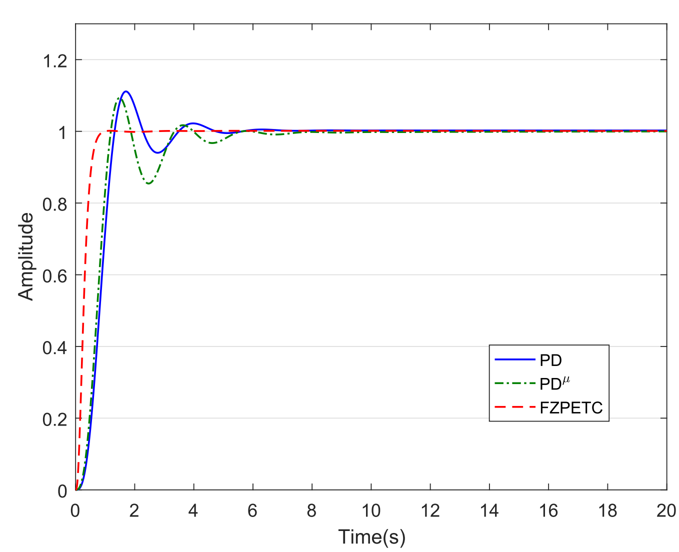

Fig. 14. Tracking performance comparison (unit step input).

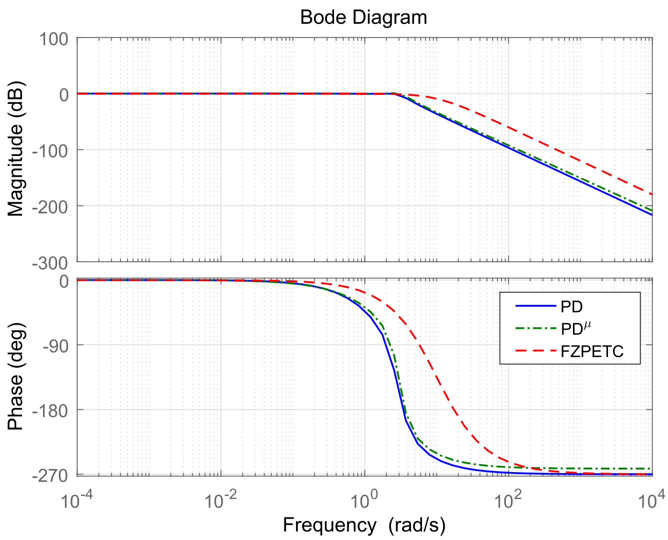

Fig. 15. Comparison of closed-loop Bode diagrams.

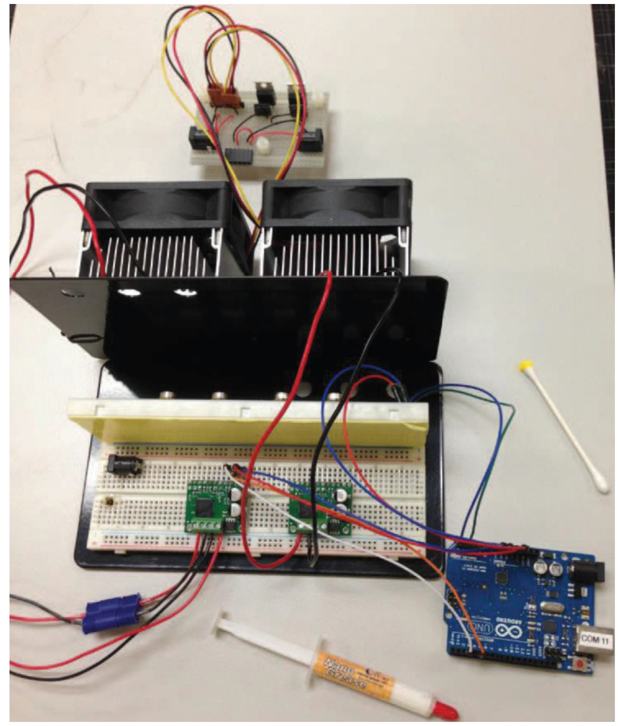

Fig. 17. Configuration of peltier plate platform.

idates the superiority of the system controlled by FZPETC. Fig. 16 shows the tracking performance comparison of a sinusoidal input ($1.3\sin(t+\frac{\pi}{6})$). The amplitude of the tracking trajectory controlled by the quasi-perfect FZPTEC is accurate, but the phase is a little off. However, the tracking performances of the system with the other two controllers fail a lot in both amplitude and phase. Though the tracking performance of the system controlled by the proposed control algorithm is not completely perfect, but it has been improved a lot compared with those controlled by the other two controllers. Meanwhile, the improper expression problem is solved and the system controlled by the quasi-perfect FZPETC will not be sensitive to high frequency disturbance.

6. Experiment

In this section, the practicality of the proposed quasi-perfect FZPETC control scheme is validated on a thermal peltier hardware-in-the-loop experimental platform. The configuration of the peltier platform is shown in Fig. 17 [32]. There are two peltier modules in the system. Each of them is attached with a fan. The fans will be maintained at a certain blowing speed when the peltiers are working. An H-bridge circuit is set between each set of peltier and fan to actuate the peltier. Four non-contact thermal sensors namely '5B, 5C, 5D, 5E' are installed oppositely to the mental plate to monitor the temperature change on the plate as shown in Fig. 18. The lower layer control unit is an Arduino Uno board based on the Atmega328p-pu microchip. The upper layer control action is done in Matlab/Simulink. So that it is a typical hardware-in-the-loop platform.

The platform is originally a two-input-four-output system, but we only focus on single-input-single-output FO controlled plant, so we only use the left peltier and sensor '3C' in our experiment. As mentioned in Ref. [32], the platform is essentially a nonlinear system, but it can be approximated as a fractional-order transfer function when the temperature changes in a small scale. Since we only use one peltier and one sensor, there is no coupling problem in the system. So the fitting model is a little different in gain and time constant compared with that in Ref. [32]. Then, we first make system identification of the unit step response of the system. The fitting model is achieved as Equation (28), and the model fitted curve and raw data are shown in Fig. 19. It can be seen that the fitting model is quite accurate.

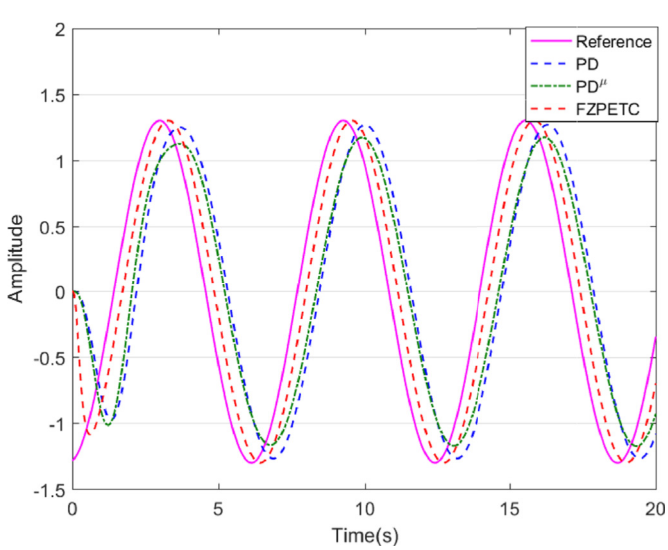

Fig. 16. Tracking performance comparison (sinusoidal input).

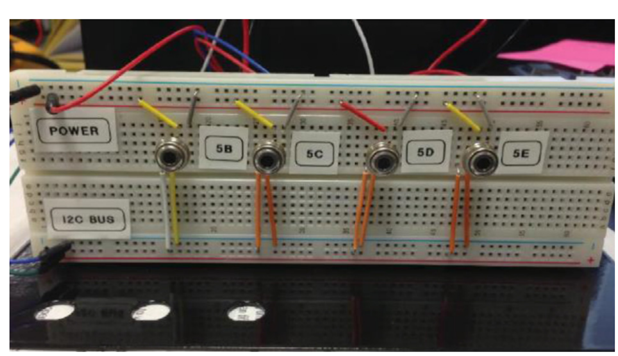

Fig. 18. Thermal sensors of the peltier plate platform.

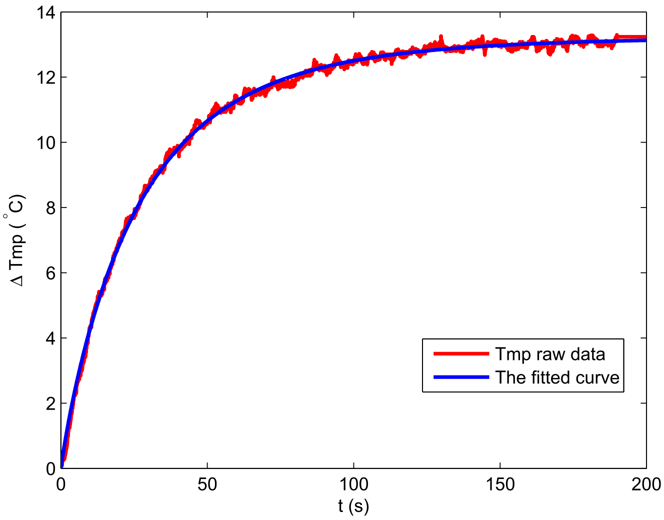

Fig. 19. Fitting model and raw data.

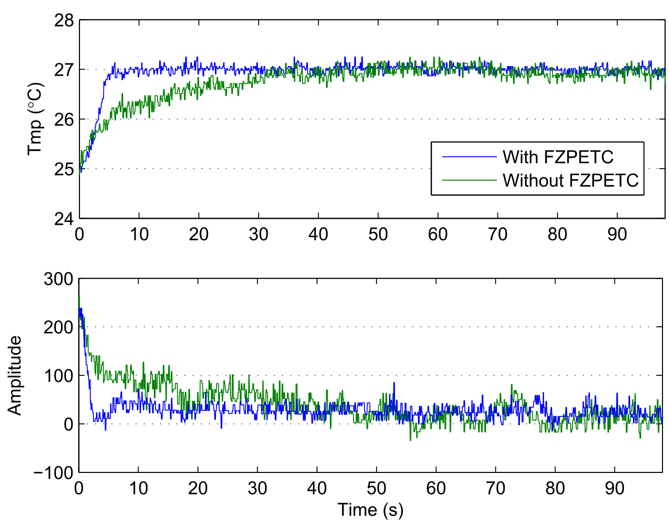

Fig. 20. Comparison of profile tracking performance (upper) and control signals (lower).

$$G_f(s) = \frac{0.1385}{23.59s^{0.9} + 1}. \tag{28}$$

In this case, we first use a controller $C_p(s)$ as below to regulate the system:

$$C_p(s) = 13.3 + \frac{0.56}{s}. \tag{29}$$

If we design the feedforward controller $F_p(s)$ according to Equation (5), the transfer function of the controller will be improper. Hence, according to the quasi-perfect method addressed in section 5, the overall transfer function $T_{p_i}(s)$ is set as Equation (30) to avoid this problem.

$$T_{p_i}(s) = \frac{1}{2.7s + 1}. \tag{30}$$

The ambient temperature where the platform is working is about 25 °C, and our target tracking temperature is 27 °C. The system is quite sensitive to tracking target change, so we just make comparison of the tracking performances of a simple step change. The comparisons of the platform control performances and control signals with and without FZPETC are demonstrated in Fig. 20. It can be seen from Fig. 20 that the tracking performance of system with FZPETC

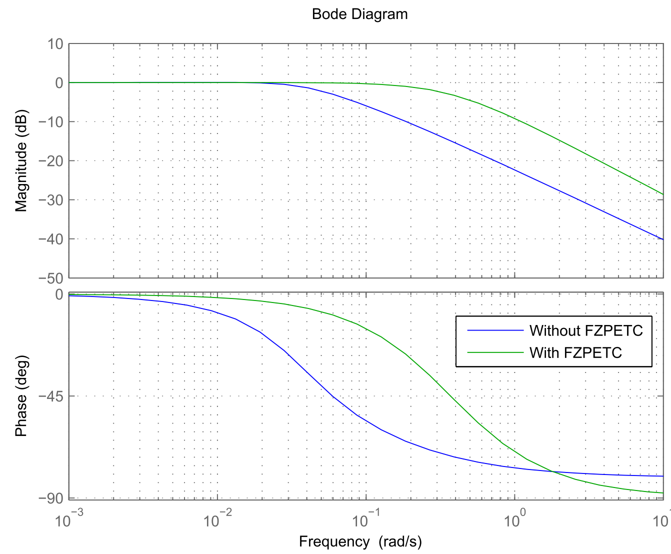

Fig. 21. Comparison of closed-loop bandwidth.

outperforms that of system without FZPETC a lot, though it is still not perfect. This kind of quasi-perfect performance exists most of time in practical situations. It is hard to get perfect tracking performance in practical experiments because there are always some physical limitations in controlled systems. The closed-loop bandwidth comparison is presented in Fig. 21. It shows that the closed-loop bandwidth of the system with FZPETC is much wider than that without FZPETC, and this is also the reason of the faster tracking speed in Fig. 20. The result verifies that the quasi-perfect FZPETC control algorithm is effective when used in practical experiment.

7. Conclusion

This paper proposes a kind of fractional-order trajectory tracking control strategy named FZPETC. This controller design algorithm can achieve zero phase shift between the desire input signal and actual output signal based on zero-pole cancellation. More accurate tracking performance will be achieved after applying the proposed controller. The controlled systems with cancellable and non-cancellable zeros have different design algorithms since the non-cancellable zeros cannot be inverted directly. Future desired trajectory information is needed because the presented feedforward controller is improper. Moreover, if the perfect tracking cannot be achieve due to some limitations and high frequency disturbance problems, a quasi-perfect tracking scheme is presented as an alternative option. Some simulation examples and a hardware-in-the-loop experiment result are given to demonstrate the effectiveness of the proposed control scheme. In the future work, we will devote our efforts to adaptive FZPETC tracking algorithm and FZPETC design for MIMO (Multi-Input-Multi-Output) fractional-order systems. Besides, the compensation method of the gain and phase error caused by different frequency components in the input signal will also need to be further considered.

References

[1] Hilfer R. Applications of fractional calculus in physics. World Scientific; 2000.
[2] Xiong JJ, Zheng EH. Position and attitude tracking control for a quadrotor uav. ISA (Instrum Soc Am) Trans 2014;53(3):725–31.
[3] Li H, Luo Y, Chen Y. A fractional order proportional and derivative (FOPD) motion controller: tuning rule and experiments. IEEE Trans Contr Syst Technol 2010;18(2):516–20.
[4] Tseng CC. Design of FIR and IIR fractional order simpson digital integrators. Signal Process 2007;87(5):1045–57.

Please cite this article in press as: Liu L, et al. Continuous fractional-order Zero Phase Error Tracking Control, ISA Transactions (2018), https://doi.org/10.1016/j.isatra.2018.01.025

[5] Chen Y. Ubiquitous fractional order controls. Proceedings of the 2nd IFAC Workshop on fractional differentiation and its applications, vol. 2. 2006.
[6] Oldham KB, Spanier J, Ross B. Fractional Calculus. Academic Press, Collier Macmillan Ltd; 1974.
[7] Monje CA, Chen Y, Vinagre BM, Xue D, Feliu-Batlle V. Fractional-order systems and controls: fundamentals and applications. Springer Science & Business Media; 2010.
[8] Podlubny I. Fractional-order systems and $PI^{\lambda}D^{\mu}$-controllers. IEEE Trans Automat Contr 1999;44(1):208–14.
[9] Liu L, Pan F, Xue D. Variable order fuzzy fractional PID controller. ISA Trans 2015;55:227–33.
[10] Zhang S, Yu Y, Wang H. Mittag-leffler stability of fractional-order hopfield neural networks. Nonlinear Anal Hybrid Syst 2015;16:104–21.
[11] Wei Y, Tse PW, Yao Z, Wang Y. Adaptive backstepping output feedback control for a class of nonlinear fractional order systems. Nonlinear Dynam 2016;86(2): 1–10.
[12] Jayasuriya S, Tomizuka M. Generalized feedforward controllers, perfect tracking and zero phase error. In: Proceedings of the 4th USA-Japan symposium on flexible automation. 1992.
[13] Park HS, Chang PH, Lee DY. Continuous zero phase error tracking controller with gain error compensation. In: Proceedings of the 1999 American Control Conference, vol. 5. IEEE; 1999. p. 3554–8.
[14] Piazzi A, Visioli A. Optimal inversion-based control for the set-point regulation of nonminimum-phase uncertain scalar systems. IEEE Trans Automat Contr 2001;46(10):1654–9.
[15] Tomizuka M. Zero phase error tracking algorithm for digital control. J Dyn Syst Meas Contr 1987;109(1):65–8.
[16] Torfs D, De Schutter J, Swevers J. Extended bandwidth zero phase error tracking control of nonminimal phase systems. J Dyn Syst Meas Contr 1992;114(3):347–51.
[17] Haack B, Tomizuka M. The effect of adding zeroes to feedforward controllers. J Dyn Syst Meas Contr 1991;113(1):6–10.
[18] Tsao TC, Tomizuka M. Adaptive zero phase error tracking algorithm for digital control. J Dyn Syst Meas Contr 1987;109(4):349–54.
[19] Adnan R, Samad AM, Tahir NM, Rahiman MHF, Mustafa MM. Trajectory zero phase error tracking control using comparing coefficients method. In: Proceedings of the 5th international colloquium on signal processing & its applications. IEEE; 2009. p. 385–90.
[20] Petras I. Stability of fractional-order systems with rational orders, fractional calculus & applied analysis. Int J Theor Appl 2009;12:269–98.
[21] Bonnet C, Partington JR. Coprime factorizations and stability of fractional differential systems. Syst Contr Lett 2000;41(3):167–74.
[22] Matignon D. Stability results for fractional differential equations with applications to control processing. In: Proceedings of computational engineering in systems applications, vol. 2. citeseer; 1996. p. 963–8.
[23] Petrás I, Chen Y, Vinagre BM. In: Robust stability test for interval fractional order linear systems, vol. 6. Princeton University Press; 2004.
[24] Zhang S, Yu Y, Wang Q. Stability analysis of fractional-order Hopfield neural networks with discontinuous activation functions. Neurocomputing 2016;171(C):1075–84.
[25] Senol B, Ates A, Alagoz BB, Yeroglu C. A numerical investigation for robust stability of fractional-order uncertain systems. ISA (Instrum Soc Am) Trans 2014;53(2):189–98.
[26] Fortuna L, Arena P, Caponetto R, Porto D. Nonlinear noninteger order circuits and systems. an introduction. World Sci. 2001.
[27] LePage WR. Complex Variables and the Laplace Transform for Engineers. McGraw-Hill, Inc., 1961 (Dover Publications, Inc., 1980).
[28] Karimi-Ghartemani M, Merrikh-Bayat F. Necessary and sufficient conditions for perfect command following and disturbance rejection in fractional order systems. In: Proceedings of the 17th IFAC world congress (IFAC'08), seoul, Korea. 2008. p. 364–9.
[29] Merrikh-Bayat F, Afshar M, Karimi-Ghartemani M. Extension of the root-locus method to a certain class of fractional-order systems. ISA (Instrum Soc Am) Trans 2009;48(1):48–53.
[30] Li Z, Liu L, Dehghan S, Chen Y, Xue D. A review and evaluation of numerical tools for fractional calculus and fractional order controls. Int J Contr 2016:1–17.
[31] Zhang M, Lin X, Yin W. An improved tuning method of fractional order proportional differentiation (FOPD) controller for the path tracking control of tractors. Biosyst Eng 2013;116(4):478–86.
[32] Li Z, Zhao T, Chen Y. A low cost research platform for modeling and control of multi-input multi-output fractional order dynamic systems. In: Proceedings of the 2014 international conference on fractional differentiation and its applications (ICFDA). IEEE; 2014. p. 1–6.

Please cite this article in press as: Liu L, et al. Continuous fractional-order Zero Phase Error Tracking Control, ISA Transactions (2018), https://doi.org/10.1016/j.isatra.2018.01.025